

Sea urchin feeding fronts

Edward R. Abraham¹

*National Institute of Water and Atmospheric Research (NIWA), P.O. Box 14-901,
Kilbirnie, Wellington, New Zealand*

Abstract

Sea urchin feeding fronts are a striking example of spatial pattern formation in an ecological system. If it is assumed that urchins are asocial, and that they move randomly, then the formation of these dense fronts is an apparent paradox. The key lies in observations that urchins move further in areas where their algal food is less plentiful. This naturally leads to the accumulation of urchins in areas with abundant algae. If urchin movement is represented as a random walk, with a step size that depends on algal concentration, then their movement may be described by a Fokker-Planck diffusion equation. For certain combinations of algal growth and urchin grazing, travelling wave solutions are obtained. Two dimensional simulations of urchin algal dynamics show that an initially uniformly distributed urchin population, grazing on an alga with a smoothly varying density, may form a propagating front separating two sharply delineated regions. On one side of the front algal density is uniformly low, and on the other side of the front algal density is uniformly high. Bounds on when stable fronts will form are obtained in terms of urchin density and grazing, and algal growth.

Email address: edward@dragonfly.co.nz (Edward R. Abraham).

¹ Present address: Dragonfly, 10 Milne Terrace, Island Bay, Wellington, New

1 Introduction

2 Dense, linear aggregations of sea-urchins are sometimes seen. These features,
known as feeding-fronts, generally occur at the boundary between grazed and
4 ungrazed habitat (Dean et al., 1984; Scheibling et al., 1999; Alcoverro, 2002;
Gagnon et al., 2004). The fronts propagate slowly towards the ungrazed re-
6 gion. Because of the high urchin densities, they are often destructive. A strik-
ing example was an aggregation of the urchin *Lytechinus variegatus*, observed
8 invading sea-grass habitat in Florida Bay (Maciá and Lirman, 1999). The ag-
gregation was estimated to be 2 - 3 m wide and 4 km long, with a density of
10 order 100 urchins m^{-2} . It is reported to have moved at a rate of up to 6 m
day⁻¹, reducing above-ground seagrass to less than 2% of its initial biomass.
12 Although it became more diffuse with time, the front remained as a coherent
feature for at least 10 months. Similar features have been seen in other benthic
14 invertebrates. Linear aggregations of starfish have been recorded invading ex-
tensive mussel beds (Dare, 1982), and traveling fronts of strombid conch have
16 also been observed in the Caribbean (Stoner, 1989; Stoner and Lally, 1994)
and in Australia (A. MacDiarmid, pers. comm.). Because of the strong influ-
18 ence of such aggregations on the benthic habitat, it is interesting to question
how they are formed and maintained.

20 Herds, flocks, schools, and swarms are all aggregations of social animals. The
aggregation is caused by the interaction between the individuals, which at-
22 tracts them together at large distances (Okubo, 1980). For animals such as
sea-urchins there is little evidence that they are social. In uniform habitat their
24 clumping is mild (Andrew and Stocker, 1986; Hagen, 1995). Experiment sug-
gests that urchins will aggregate in the presence of food (Vadas et al., 1986),
Zealand (www.dragonfly.co.nz)

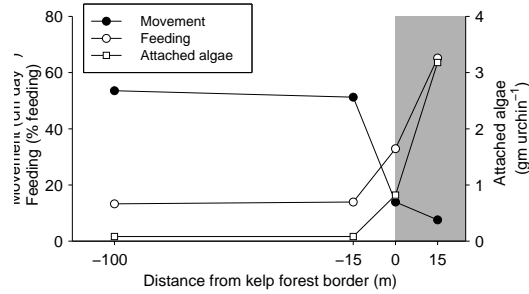


Fig. 1. Movement of red sea urchins, *Strongylocentrotus franciscanus*, near the boundary of a kelp forest at Santa Cruz Point (redrawn from Mattison et al., 1977). The figure shows the average rate of urchin movement, measured over a 24 hour period, at four locations. For comparison, the percentage of urchins which were observed to be feeding, and the weight of algae attached to the urchins' oral surface, are also shown. Within the kelp forest (shaded), feeding is high and movement rates are low.

26 but there is no evidence for a strong social interaction. Moreover, studies
of urchin movement have found that while they may exhibit a chemosen-
28 sory response to algae, they do not show any directed movement towards it
(Andrew and Stocker, 1986). A recent flume tank study shows that the urchin
30 *Lytechinus variegatus* can move in a directed manner towards a food source
under some flow conditions (Pisut, 2002). This may explain how urchins lo-
32 cate their food at short distances. Both the flow and the chemical signals
are likely to be more complex in the urchins' natural environment. In field
34 studies the direction of urchin movement is usually found to be either ran-
dom or weakly directional (Duggan and Miller, 2001; Dumont et al., 2006;
36 Lauzon-Guay et al., 2006). The question then is how to explain the formation
of intense aggregations in an asocial animal, which appears not to be able to

38 move in a directed manner.

A recurrent observation is that there is an inverse relation between urchin
40 movement and macrophyte density (Mattison et al., 1977; Andrew and Stocker,
1986; Dance, 1987; Dumont et al., 2006). A study by Mattison et al. (1977) of
42 red sea-urchins (*Strongylocentrotus franciscanus*) near Santa Cruz found that
urchins within a kelp forest moved by 7.5 cm day^{-1} , whereas outside it the
44 movement rate increased to over 50 cm day^{-1} (Fig. 1). The reasons for the dif-
ference in movement rates between habitats is not clear. Some studies find that
46 movement rate is more for starved urchins (Dix, 1970; Hart and Chia, 1990),
whereas others find either no effect (Dumont et al., 2006) or the opposite rela-
48 tion (Klinger and Lawrence, 1985). It has also been shown, by using physical
models of large algae, that the movement of foliose algae by the water may
50 restrict urchin movement (Konar and Estes, 2003). In this paper, the conse-
quences of differential motility in different habitats will be explored, whatever
52 its cause. Four simple assumptions are made about sea urchin movement:

- (1) Sea urchins are asocial, with the movements of individual urchins being
54 independent
- (2) The direction of sea urchin movement is random (over a suitable time
56 period, which we take to be 24 hours)
- (3) The sea-urchin movement rate decreases as the macrophyte density in-
58 creases
- (4) The distance moved in a 24 hour period is related to the seaweed density
60 at the beginning of the time-period.

The consequences of these assumptions are explored, using both analytical
62 techniques and direct simulation. It might seem to be intuitively reasonable

that if the urchins are randomly moving then they will disperse, and it will be
64 impossible for them to accumulate into an organised structure like a feeding
front. In this paper it is shown that under certain circumstances, and with a
66 suitable representation of macrophyte growth and urchin grazing, the assump-
tions about urchin movement may lead to persistent urchin feeding fronts.

68 There are other features of urchin movement which are not accounted for by
this model. A recent study (Lauzon-Guay et al., 2006) of sea urchin movement,
70 which followed the movements of individual urchins using video techniques,
showed that the distance moved decreased with increasing urchin density.
72 This effect is not included in the present study. Other authors have con-
cluded that the urchin response to predators may mediate the formation
74 of feeding fronts (Bernstein et al., 1981). The model we discuss is a mini-
mal model. The complexities of differential feeding on multi species algal as-
76 semblages (Gagnon et al., 2004; Wright et al., 2005), size dependent urchin
movement (Dumont et al., 2004, 2006), seasonal variations in movement rate
78 (Konar and Estes, 2001; Dumont et al., 2004), relation between behaviour and
the supply of drift algae (Dayton et al., 1984), interactions between movement
80 and the substrate (Laur et al., 1986), or between water movement and urchin
movement (Kawamata, 1998) are not included. All demographic processes
82 such as urchin growth, recruitment and mortality have also been ignored. If
sufficient data were available these processes could be represented. However,
84 while their inclusion would lead to a more realistic model of a specific system,
the purpose of this paper is to explore the consequences of a single urchin

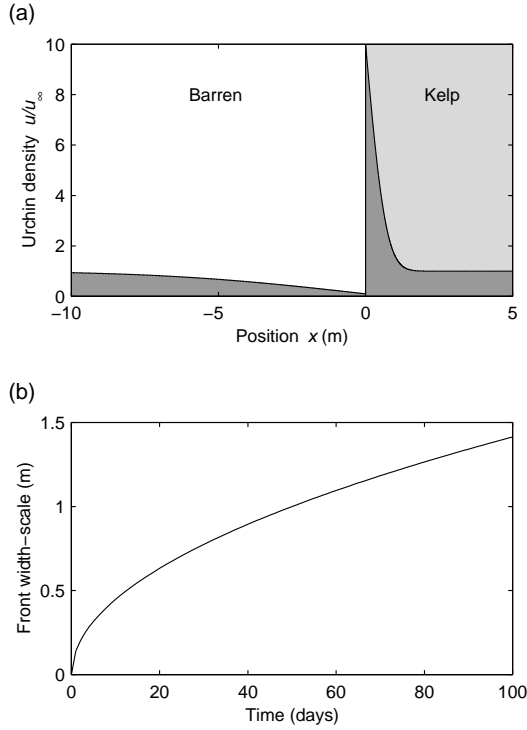


Fig. 2. Solution to the Fokker-Planck equation, eq. (2), describing the dispersal of an initially uniform population of sea-urchins in response to a step-change in macrophyte density. The right-hand side, $x > 0$, is kelp forest with the urchin movement being $\lambda_+ = 0.1$ m and the left-hand side, $x < 0$, is barren with $\lambda_- = 1$ m (here $\Delta t = 1$ day). These values are chosen to be comparable with Mattison et al. (1977). (a) The urchin distribution after 30 days, with the initial population having a value $u/u_\infty = 1$. There is a net movement of urchins from the barren region to the kelp-forest, with a sharp peak appearing at the kelp boundary. (b) The width of the peak, $2\sqrt{D_+t}$, increases very slowly. Even after 100 days it is less than two meters wide. The maximum urchin density is constant with time, at 10 times the initial population.

86 behaviour.

2 Urchin movement and the Fokker-Planck equation

88 The four assumptions above may be used to formalize sea-urchin movement as a random walk. If $x_i(t)$ is the position of urchin i at time t , then its position

90 a time Δt later may be represented as

$$x_i(t + \Delta t) = x_i(t) + \eta(t)\lambda(s(x_i(t))), \quad (1)$$

92 where $\eta(t)$ is a dimensionless random variable with a zero mean and a unit
variance, and $\lambda(s(x))$ (dimensions $[x]$) is a characteristic step-size which is a
94 function of the macrophyte density, s .

If the movement of individual sea urchins satisfies eq. (1), then the disper-
96 sal of the population may be approximated by the continuous Fokker-Planck
equation (Turchin, 1998),

$$98 \quad \frac{\partial u}{\partial t} = \frac{\partial^2}{\partial x^2}(Du), \quad (2)$$

where $u(x, t)$ is the urchin density and the motility $D(s)$ (dimensions $[x^2 t^{-1}]$)
100 is related to the random-walk parameters by

$$D(s) = \frac{\lambda(s)^2}{2\Delta t}. \quad (3)$$

102 The long term behavior of the population u is well-known. If the total number
of sea-urchins is constant with time, then the steady state solution to eq. (2)
104 is

$$u(x, t) = c/D(s), \quad (4)$$

106 where c is a constant. At equilibrium, the population density will be inversely
related to the motility. The sea-urchins will accumulate in areas where the
108 seaweed concentration is higher, and so the individual urchins are moving
more slowly. The aggregation of randomly walking foragers in regions with

110 higher food density, is known variously as preytaxis (Kareiva and Odell, 1987),
 112 orthokinesis (Okubo, 1980), or phagokinesis (Andrew and Stocker, 1986). An
 114 experimental study of ladybugs feeding on an inhomogeneous aphid population
 showed that, in this case, eq. (4) provided a good description of the data
 (Turchin, 1998). The random walk formalism is similar to (although simpler
 than) that used to understand the formation of traveling bands of bacteria
 116 through chemotaxis (Keller and Segel, 1971).

While it has been observed that urchin movement is higher when the algal
 118 density is lower, little is known about the functional form of $\lambda(s)$. In the
 absence of any data, we will simply assume that there is a threshold algal
 120 density, s_c , at which the rate of urchin movement changes from a minimum to
 a maximum value,

$$122 \quad D = \begin{cases} D_-, & s < s_c \\ D_+, & s \geq s_c \end{cases}, \quad (5)$$

where $D_- > D_+ > 0$. Within this model, the urchins have only two behaviours.
 124 This simplifying assumption has the advantage of making analytic solutions
 to the Fokker-Plank equation possible.

126 **3 Analytical solutions**

3.1 Solving for a fixed boundary

128 As a first step towards understanding the formation of feeding-fronts, the
 response of an urchin population to a step-change in the motility is considered.

130 The boundary between the barren and the kelp regions is assumed to be fixed,
 with the macrophyte density being greater than the critical density, s_c , for
 132 $x > 0$ and less than s_c for $x \leq 0$. It follows from eq. (5) that the motility
 is $D = D_+$, ($x > 0$) and $D = D_-$, ($x \leq 0$), where $D_{\pm} = \lambda_{\pm}^2/2\Delta t$. If it is
 134 assumed that the urchin population is initially uniformly distributed, then
 $u(x, 0) = u_{\infty}$, where u_{∞} is a constant.

136 Away from the boundary between the two regions, the motility is constant and
 eq. (2) reduces to a diffusion equation. If we write $u(x, t) = u_+(x, t)$, ($x \geq 0$)
 138 and $u(x, t) = u_-(x, t)$, ($x < 0$) then, for the derivatives on the right hand side
 of eq. (2) to be continuous, we require that

$$140 \quad D_+u_+(0, t) = D_-u_-(0, t). \quad (6)$$

We will look for a solution which has both $u_+(0, t)$ and $u_-(0, t)$ constant with
 142 time, and so will require that $\partial^2(Du)/\partial x^2|_{x=0} = 0$. Because the total urchin
 population is constant, any increase in the urchin density at positive x must
 144 be matched by a decrease in density at negative x ,

$$\int_0^{\infty} (u_+ - u_{\infty})dx = \int_{-\infty}^0 (u_{\infty} - u_-)dx. \quad (7)$$

146 The solution to a diffusion equation with a constant boundary is given by the
 complementary error function,

$$148 \quad \text{erfc}(x) = 1 - \frac{1}{\sqrt{\pi}} \int_0^x e^{-\beta^2} d\beta, \quad (8)$$

with β being an integration constant. The solution for the urchin population
 150 may be written as

$$u_{\pm}(x, t) = u_{\infty} \left(1 \mp \gamma_{\pm} \operatorname{erfc} \left(|x|/2\sqrt{D_{\pm}t} \right) \right), \quad (9)$$

152 where γ_{\pm} are constants which must satisfy

$$D_+\gamma_+ + D_-\gamma_- = D_+ - D_- \quad (10)$$

154 in order to solve eq. (6). For eq. (7) to hold,

$$\gamma_+/\gamma_- = \sqrt{D_-/D_+}. \quad (11)$$

156 With this ratio $\partial^2 Du/\partial x^2|_{x=0} = 0$, and the Fokker-Planck equation is solved throughout the domain. From eqs. (10) and (11) it follows that

$$158 \quad \gamma_{\pm} = \frac{D_+ - D_-}{\sqrt{D_{\pm}}(\sqrt{D_-} + \sqrt{D_+})}. \quad (12)$$

A plot of the solution is given in fig. (2). The initially uniform urchin density
 160 develops a peak at the boundary between the two regions. There is an increased
 urchin density just inside the kelp, and a depleted region on the barren side
 162 of the boundary. The height of the peak is constant with time, but the width
 grows steadily. On the barren side of the peak there is a region where the
 164 sea-urchin density is less than the initial value.

3.2 Solving for a moving boundary

166 We now look for traveling wave solutions of the Fokker-Planck equation, repre-
 senting a steadily moving urchin front. At this stage, the grazing of the urchins
 168 is not considered, it is simply assumed that the boundary between the two
 regions moves at a constant velocity c . The variable $z = x - ct$ is introduced.
 170 The traveling solutions are functions of z only, and they satisfy the equation,

derived from eq. (2),

$$-c \frac{du}{dz} = \frac{d^2 Du}{dz^2}, \quad (13)$$

where $u = u(z)$ and $D = D(z)$. If the boundary between the grazed and ungrazed regions falls at $z = 0$, the motility is

$$D(z) = \begin{cases} D_-, & z \leq 0 \\ D_+, & z > 0 \end{cases}. \quad (14)$$

By integrating eq. (13) twice, an integral equation for the urchin density is obtained,

$$D(z)u(z) = -c \int_{-\infty}^z (u(x) - u_\infty) dx + D_- u_\infty, \quad (15)$$

where the constant of integration, u_∞ , has been chosen so that $u(\pm\infty) = u_\infty$.

It is straightforward to verify that the solution to eq. (15) is given by the function

$$\frac{u(z)}{u_\infty} = \begin{cases} 1, & z \leq 0 \\ \frac{D_- - D_+}{D_+} e^{-cz/D_+} + 1, & z > 0 \end{cases}. \quad (16)$$

If the motility is larger in the grazed region, $D_- > D_+$, then the traveling wave solution has the form of a feeding front, with a peak at the boundary between the regions. The maximum density within the feeding front occurs on the boundary, with a density $u_\infty D_- / D_+$. The urchin density is constant throughout the barren region, and decays exponentially towards the ungrazed

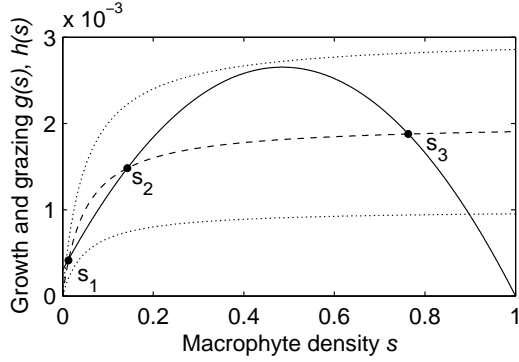


Fig. 3. Variation in macrophyte growth $g(s)$ (solid line) and urchin grazing $h(s)$ (dashed line) as a function of the macrophyte density, s . The curves follow eqs. (21, 22), with the parameters $\mu_s = 0.01 \text{ day}^{-1}$; $s_0 = 0.03 s_{\max}$; $k_s = 0.05 s_{\max}$; $\alpha = 0.001 s_{\max} \text{ urchin}^{-1} \text{ day}^{-1}$. The dashed line is drawn for an urchin density of $u_\infty = 2 \text{ urchin m}^{-2}$. The three intersection points of $g(s)$ and $h(s)$ are labeled by the macrophyte densities s_1 , s_2 and s_3 . The upper and lower dotted lines show the urchin grazing with the same parameters, but with urchin densities of $u_\infty = 3 \text{ urchin m}^{-2}$ and $u_\infty = 1 \text{ urchin m}^{-2}$, respectively. With these densities there is only one solution of $ds/dz = 0$ (eq. 18), and so there are no possible traveling wave solutions that could represent an urchin feeding-front.

188 side of the boundary, the front having a width of D_+/c .

The feeding front can only propagate continually if there is a non-zero urchin
 190 density within the ungrazed region. Otherwise, the front will lose urchins as
 it travels and decay away.

192 4 Introducing seaweed

Having identified a frontal solution to the urchin density when the boundary
 194 is moving steadily, the question is whether there are traveling wave solutions
 to the coupled seaweed-urchin equations. The change in algal density is taken
 196 to occur through a combination of growth and grazing,

$$\frac{\partial s}{\partial t} = g(s) - h(s)u, \quad (17)$$

198 where $g(s)$ describes the algal growth and $h(s)u$ is the grazing rate of the
 urchins on the seaweed. There is no explicit seaweed dispersal included. Re-
 200 cruitment from a wider seaweed population is simply represented by a non-zero
 intercept of $g(s)$. For a traveling wave solution to exist, s must be a function
 202 of $z = x - ct$ only, so

$$\frac{\partial s}{\partial z} = h(s)u/c - g(s)/c. \quad (18)$$

204 At $z = \pm\infty$ the population must be in equilibrium, $h(s)u_\infty = g(s)$, with
 $s(\infty) > s_c$ and $s(-\infty) \leq s_c$. There must be at least three real, positive
 206 solutions to

$$\partial s / \partial z |_{u=u_\infty} = 0, \quad (19)$$

208 which we shall call s_1 , s_2 , and s_3 ($s_3 > s_2 > s_1$). The solutions s_1 and s_3 are
 stable, and s_2 is unstable. In order that $s < s_c$ for $z < 0$ it is required that

$$210 \quad s_2 > s_c > s_1. \quad (20)$$

If this does not hold then no traveling wave solutions can be obtained. The
 212 propagation speed can be obtained by requiring that $s = s_c$ at $z = 0$, where
 the urchin density, u , in eq. (18) is obtained from eq. (16).

214 As a plausible example, assume that macrophyte growth is logistic

$$g(s) = \mu_s(s + s_0)(1 - s/s_{\max}), \quad (21)$$

216 where μ_s (dimensions $[t^{-1}]$) is the growth-rate s_{\max} (dimensions $[s]$) is the
 218 macrophyte carrying capacity and the term $\mu_s s_0$ (dimensions $[st^{-1}]$) repre-
 220 to a maximal density will take a time of order μ_s^{-1} .

An appropriate representation of grazing is the Holling type II or Michaelis-
 222 Menten equation (Holling, 1959; Begon et al., 1996)

$$h(s) = \frac{\alpha s}{s + k_s}, \quad (22)$$

224 where α (dimensions $[su^{-1}t^{-1}]$) parameterizes the maximal grazing rate per
 urchin, and k_s (dimensions $[s]$) is the half-saturation constant for urchin graz-
 226 ing. At low algal densities the grazing function decreases to zero, representing
 the difficulty that urchins have in locating food when the macrophyte is sparse.

228 As an example, growth parameters relevant to the New Zealand alga *Ecklonia*
radiata are used. This species grows to a mature size within a year, and so
 230 an order-of-magnitude growth-rate is estimated to be $\mu_s = 0.01 \text{ day}^{-1}$. The
 recruitment density s_0 will be site specific, depending on the abundance of
 232 mature alga in the surrounding area. It is simply assumed that s_0 is a small
 fraction of the maximum density, $s_0 = 0.03s_{\max}$. An estimate of urchin grazing
 234 rates may be obtained from the results of a small experiment carried out by
 Russell Cole (1993). A square meter quadrat was loaded with urchins (*Evechi-*
 236 *nus chloroticus*), to a density of 60 m^{-2} , and the decrease in the abundance of
 the alga *E. radiata* was monitored. Even at this high urchin density the decline
 238 in alga was slow, with a time-scale of ~ 20 days. The maximum grazing rate is
 therefore $\alpha = 1/(20 \times 60) = 0.001 s_{\max} \text{ urchin}^{-1} \text{ m}^2 \text{ day}^{-1}$. The algal density

240 at which the urchin grazing is half of its maximum is taken to be $k_s = 0.1s_{\max}$.

In the absence of any data on the variation of urchin motility with algal concentration, it will simply be assumed that the critical algal density is $s_c = k_s$.

The growth and grazing curves that result from these parameters are shown in fig. (4), for three differing urchin densities. Detailed experiment would be needed to verify both the functional form and the parameterization of the growth and grazing functions. The intent here is to illustrate the qualitative features of the urchin-macrophyte system, rather than quantitative modeling of a specific case.

The existence of three solutions to eq. (19) could be determined by directly solving this cubic equation. While analytically tractable, the general solution will be complicated. A more amenable estimate of when three real, positive solutions can be found is readily obtained by graphical inspection of the growth and grazing functions, $g(s)$ and $h(s)$. If the recruitment density s_0 is zero, then three solutions to eq. (19) will only be found if the initial slope of the grazing function is larger than the initial slope of the growth function. This will only hold if

$$u_\infty > \frac{\mu_s k_s}{\alpha}. \quad (23)$$

258 If $k_s \ll s_{\max}$, then the maximal grazing rate also needs to be less than the maximal growth rate. This implies that

$$260 \quad u_\infty < \frac{\mu_s s_{\max}}{4\alpha}. \quad (24)$$

Both of these inequalities, (23) and (24), can only be satisfied simultaneously if

$$k_s < s_{\max}/4. \tag{25}$$

264 If the recruitment density s_0 is non-zero but small, $s_0 \ll s_{\max}$, then these
 conditions will still be relevant. For the parameters used in fig. (4) the con-
 266 ditions given in eqs. (23, 24) translate to the requirement that 1 urchin m^{-2}
 $< u_\infty < 2.5 \text{ urchin m}^{-2}$. These are not exact bounds, but they provide a useful
 268 estimate of the range over which three solutions to eq. (18) can be found.

For a feeding-front solution to exist it is also necessary that the transition
 270 from high to low urchin motility occurs at a macrophyte density, s_c , which
 is between s_1 and s_2 (eq. 20). In the case presented in fig. (4), this would be
 272 satisfied by $s_c = 0.1s_{\max}$. The range of initial urchin densities over which a
 feeding front solution develops is small, with a factor of less than 3 between
 274 a density that leads to macrophyte beds and a density that results in urchin
 barrens.

276 **5 Numerical simulations**

5.1 The traveling wave

278 For comparison with the analytic solutions numerical simulations are carried
 out. The first set of simulations aims to check the validity of the traveling
 280 wave solution, eq. (16). A one dimensional model is built, which begins with
 uniformly distributed urchins, each urchin having a real-valued position. The
 282 boundary between the low and high motility regions begins at $x = 1200 \text{ m}$
 and moves towards the right at a velocity $c = 1 \text{ m day}^{-1}$. At each timestep,
 284 for each urchin, a random number η is generated from a normal distribution

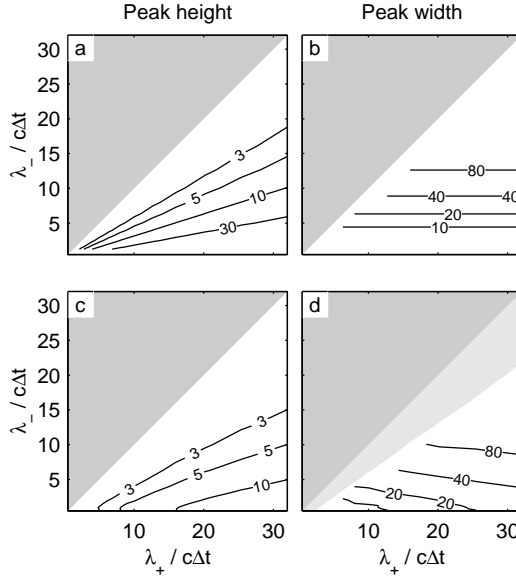


Fig. 4. Comparison between the theoretical form of a traveling wave (eq. 16) and numerical simulations, as described in section 5.1. (a) The theoretical peak height, D_-/D_+ (b) The theoretical width, D_+/c . (c) The maximum height of the peak from the simulations (d) The width of the peak. The half-shading masks the region where the peak height is too small to allow a width to be reliably calculated.

with zero mean and variance. If the urchin is to the right of the boundary it
 286 is moved by $\lambda_+\eta$. Otherwise, the urchin is moved by $\lambda_-\eta$. These rules capture
 the assumptions which led to the derivation of eq. (16). A window 800 m wide
 288 is maintained around the boundary, with a border 150 m wide beyond that.
 Urchins are added or removed from the simulation to hold the density constant
 290 within the two border regions. Any urchins which move beyond the border are
 removed. The simulation starts with a uniform density of 50 urchins m^{-1} . It is
 292 run for 2000 timesteps, with data from the final 200 timesteps being grouped
 into 1 m long bins and averaged. The whole simulation is repeated for a range
 294 of λ_+ and λ_- ($\lambda_- > \lambda_+$). A comparison of the theoretical and the numerical
 peak widths and heights are shown in fig. (5). There is good agreement between
 296 the two approaches, confirming that these simple assumptions can lead to a

propagating peak in urchin density.

298 *5.2 Two dimensional simulations with macrophyte*

Finally, a simulation is run to check the stability of the feeding fronts in a
300 two-dimensional setting, with macrophyte. A numerical domain is used which
represents a 500 m \times 500 m square, divided into 1 m² cells. Each cell has a
302 seaweed density, s , with the density going from $s = 0$ on the left hand side of
the domain to $s = s_{\max}$ on the right hand side. The seaweed distribution has
304 some initial variability, introduced by adding a random function to the linear
gradient (fig. 5.2a). The random function has greater variability at longer
306 length scales, with a Fourier transform that decays as $f^{-3/4}$, where f is the
wavenumber. This is done to introduce noise into the model, capturing in some
308 way the natural environmental variability. Urchins are then added, uniformly
distributed through the whole domain, and with an average density of 1.5
310 urchin m⁻². At each timestep the seaweed within each cell changes according
to eq. (17). A simple finite-difference approximation is used, and the seaweed
312 density is always kept above zero. The urchin density is calculated from the
number of urchins within each 1 m² cell, and the seaweed is grazed accordingly.
314 The urchins are then moved by a random amount, with the size of the step, λ ,
depending on whether the seaweed density exceeds the threshold. Any urchins
316 moving outside the domain are reflected back into it, so the total number of
urchins within the domain is constant.

318 The results are shown in fig. (5.2). In the simulations shown, the following
parameters have been used, $\lambda_+ = 0.05$ m day⁻¹; $\lambda_- = 1$ m day⁻¹; $k_s =$
320 $0.05s_{\max}$; $s_0 = 0.01s_{\max}$; $\mu = 0.01$ day⁻¹; $\alpha = 0.001s_{\max}$ urchin⁻¹ m²; and

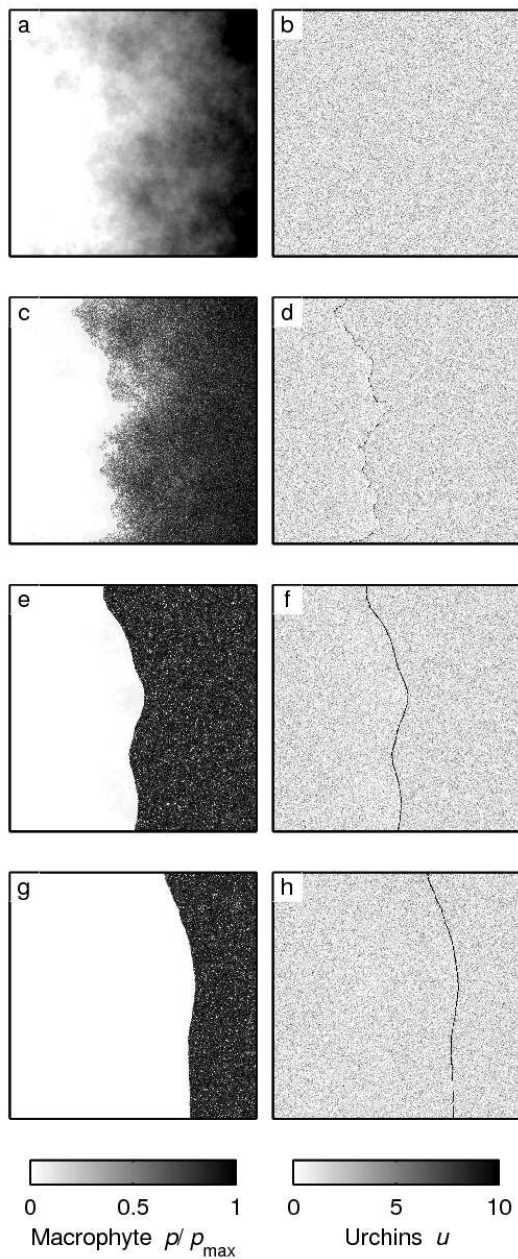


Fig. 5. Simulation of seaweed (a, c, e, g) and urchins (b, d, f, h), showing the formation of a feeding front. The pictures are made at 0 (a, b), 600 (c, d), 3000 (e, f) and 6000 (g, h) model days.

$s_c = k_s$, similar to the parameters in fig. (4). The simulations are run for
 322 10,000 model days, with the figure showing the seaweed density and the urchin
 density at 0, 600, 3000 and 6000 model days.

324 From the start of the simulation the seaweed density becomes increasingly
polarized, with areas of urchin barren, and areas of close to maximum density.
326 A feeding front develops along the boundary between the regions, and the
boundary slowly propagates towards the ungrazed region. The front appears
328 stable, becoming smoother with time.

6 Discussion

330 The simple assumptions of differential urchin movement in response to sea-
weed density lead to the formation and propagation of an urchin feeding front,
332 in qualitative agreement with observations. No social behavior needs to be as-
sumed to explain the persistence of the front, and the motion of each urchin
334 can be random. The system provides an excellent example of how simple in-
dividual processes can lead to spatial pattern. The development of the fronts
336 shows the importance of correctly representing movement. Diffusion approxi-
mations, based on Fickian diffusion, are often used to represent animal disper-
338 sal (Okubo, 1980). Because Fickian diffusion will always lead to the density
of a population decreasing (at least in the absence of any reproduction or
340 migration) it is unable to generate sharp fronts. A simple change to the rep-
resentation of dispersal, from Fickian to Fokker-Planck, leads to a model that
342 captures the qualitative features of the system. The focus of the analysis has
been on demonstrating that the system can develop a stable propagating front.
344 This simple model may also be used to explore the dynamics of more transient
phenomena, such as the effect of a localised recruitment of urchins, or how a
346 patchy mosaic of barrens and macrophyte habitat can be maintained. With
the two states that are stable to small perturbations and the transitional wave
348 transforming one to the other, the urchin-macrophyte system has many of the

features of excitable media (Murray, 1993). There is ample scope for further
350 exploration of this analogy.

With the movement rates used here, the propagation speed of the front is very
352 slow. In the two dimensional simulation, the front moved at a speed of 10 m
per model year. This is on a similar order to propagation speeds of 2.5 m
354 month⁻¹ reported from field observations (Gagnon et al., 2004). In contrast
the aggregation of *Lytechinus variegatus* in Florida Bay was reported to move
356 at 6 m day⁻¹. The propagation rate will be strongly dependent on the details of
the urchin grazing. It is likely that the assumption of asociality, or of urchin
358 independence, breaks down at the high densities encountered in the front.
Because of the very narrow spatial extent of the frontal region, the urchin
360 behavior at high densities will effect the outcome of the model. To produce a
quantitatively accurate model would require more detailed observations. Stud-
362 ies which focus on the movements of individual urchins (Lauzon-Guay et al.,
2006) are likely to generate the data required to build a better representa-
364 tion of the frontal dynamics. For example the inclusion of a traffic-jam effect,
where the movement rate of the urchins decreases as the density increases
366 (Lauzon-Guay et al., 2006), will result in an increased urchin density within
the front.

368 As discussed in the introduction, there are other processes that are known
to influence urchin behaviour which could be represented within a model of
370 this nature. Unfortunately, the effects of many of these factors have only been
measured in a few isolated experiments, and there is insufficient published data
372 to include them. The model developed here is in many ways a null model. It is
hoped that it will inspire experimentalists to collect the individual based data
374 which is needed to understand the full detail of how urchin feeding fronts are

formed and maintained.

376 **7 Acknowledgements**

I am grateful to Andrew Visser for discussions on random walks; to Russell
378 Cole for discussions on urchin biology and to Alison MacDiarmid and Alistair
Dunn for their support and encouragement. This project was funded by the
380 New Zealand Foundation for Research in Science and Technology.

References

- 382 Alcoverro, 2002. Effects of sea urchin grazing on seagrass (*Thalassodendron*
ciliatum) beds of a Kenyan lagoon. Mar. Ecol. Prog. Ser. 226, 255–263.
- 384 Andrew, N. L., Stocker, L. J., 1986. Dispersion and phagokinesis in the echi-
noid *Evechinus chloroticus* (Val.). J. Exp. Mar. Biol. Ecol. 100, 11–23.
- 386 Begon, M., Harper, J. L., Townsend, C. R., 1996. Ecology: Individuals, popu-
lations and communities, 3rd Edition. Blackwell Science, Cambridge, MA.
- 388 Bernstein, B. B., Williams, B. E., Mann, K. H., 1981. The role of behav-
ioral responses to predators in modifying urchins' (*Strongylocentrotus droe-*
390 *bachiensis*) destructive grazing and seasonal foraging patterns. Mar. Biol.
63, 39–49.
- 392 Dance, C., 1987. Patterns of activity of the sea urchin *Paracentrotus lividus* in
the Bay of Port-Cros (Var, France, Mediterranean). Mar. Ecol. 8, 131–142.
- 394 Dare, P. J., 1982. Notes on the swarming behaviour and population density
of *Asterias rubens* L. (Echindermata: Asteroidea) feeding on the mussel,
396 *Mytilus edulis* L. J. Const. int. Explor. Mer. 40, 112–118.
- Dayton, P. K., Currie, V., Gerrodette, T., Keller, B. D., Rosenthal, R., Ven
398 Tresca, D., 1984. Patch dynamics and the stability of some California kelp

- communities. Ecol. Monogr. 54, 253–289.
- 400 Dean, T. A., Schroeter, S. C., Dixon, J. D., 1984. Effects of grazing by
two species of sea urchins (*Strongylocentrotus franciscanus* and *Lytechinus*
402 *anamesus*) on recruitment and survival of two species of kelp (*Macrocystis*
pyrifera and *Pterygophora californica*). Mar. Biol. 78, 301–313.
- 404 Dix, T. G., 1970. Biology of *Evechinus chloroticus* (Echinoidea: Echinometri-
dae) from different localities. N. Z. J. Mar. Freshwat. Res. 4, 267–277.
- 406 Duggan, R. E., Miller, R. J., 2001. External and internal tags for the green
sea urchin. J. Exp. Mar. Biol. Ecol. 258, 115–122.
- 408 Dumont, C., Himmelman, J. H., Russel, M. P., 2004. Size-specific movement
of green sea urchins *Strongylocentrotus droebachiensis* on urchin barrens in
410 eastern Canada. Mar. Ecol. Prog. Ser. 276, 93–101.
- Dumont, C., Himmelman, J. H., Russel, M. P., 2006. Daily movement of the
412 sea urchin *Strongylocentrotus droebachiensis* in different subtidal habitats in
eastern Canada. Mar. Ecol. Prog. Ser. 317, 87–99.
- 414 Gagnon, P., Himmelman, J. H., Johnson, L. E., 2004. Temporal variation in
community interfaces: kelp-bed boundary dynamics adjacent to persistent
416 urchin barrens. Mar. Biol. 144, 1191–1203.
- Hagen, N. T., 1995. Recurrent destructive grazing of successional immature
418 kelp forests by green sea urchins in Vestfjorden, Northern Norway. Mar. Ecol.
Prog. Ser. 123, 95–106.
- 420 Hart, L. J., Chia, F.-S., 1990. Effect of food supply and body size on the
foraging behavior of the burrowing sea urchin *Echinometra mathaei* (de
422 Blainville). J. Exp. Mar. Biol. Ecol. 135, 99–108.
- Holling, C. S., 1959. Some characteristics of simple types of predation and
424 parasitism. Canadian Entomologist 91, 385–398.

- Kareiva, P., Odell, G., 1987. Swarms of predators exhibit “preytaxis” if indi-
426 vidual predators use area-restricted search. *Am. Nat.* 130, 233–270.
- Kawamata, S., 1998. Effect of wave-induced oscillatory flow on grazing by
428 a subtidal sea urchin *Strongylocentrotus nudus* (A. Agassiz). *J. Exp. Mar.
Biol. Ecol.* 224, 31–48.
- 430 Keller, E. F., Segel, L. A., 1971. Traveling bands of chemotactic bacteria: a
theoretical analysis. *J. theor. Biol.* 30, 235–248.
- 432 Klinger, T. S., Lawrence, J. M., 1985. Distance perception of food and the ef-
fect of food quantity on feeding behavior of *Lytechinus variegatus* (Lamarck)
434 (Echinodermata: Echinoidea). *Mar. Behav. Physiol.* 11, 327–344.
- Konar, B., Estes, J. A., 2001. Seasonal changes in subarctic sea urchin popu-
436 lations from different habitats. *Polar Biology* 24, 754–763.
- Konar, B., Estes, J. A., 2003. The stability of boundary regions between kelp
438 beds and deforested areas. *Ecology* 84, 174–185.
- Laur, D. R., Ebeling, A. W., Reed, D. C., 1986. Experimental evaluations of
440 substrate types as barriers to sea urchin (*Strongylocentrotus* spp.) move-
ment. *Mar. Biol.* 93, 209–215.
- 442 Lauzon-Guay, J.-S., Scheibling, R. E., Barbareau, M. A., 2006. Movement
patterns in the green sea urchin, *Strongylocentrotus droebachiensis*. *J. Mar.
444 Biol. Ass. U.K.* 86, 167–174.
- Maciá, S., Lirman, D., 1999. Destruction of Florida Bay seagrasses by a grazing
446 front of sea urchins. *Bull. Mar. Sci.* 65, 593–601.
- Mattison, J. E., Trent, J. D., Shanks, A. L., Akin, T. B., Pearse, J. S., 1977.
448 Movement and feeding activity of red sea urchins (*Strongylocentrotus franc-
sicanus*) adjacent to a kelp forest. *Mar. Biol.* 39, 25–30.
- 450 Murray, J. D., 1993. *Mathematical biology*, 2nd Edition. Vol. 19 of *Biomath-
ematics*. Springer-Verlag, Berlin.

- 452 Okubo, A., 1980. Diffusion and ecological problems: mathematical models.
Vol. 10 of Biomathematics. Springer-Verlag, Berlin.
- 454 Pisut, D. P., 2002. The distance chemosensory foraging behavior of the sea
urchin *Lytechinus variegatus*. Master's thesis, Georgia Institute of Technol-
456 ogy, Atlanta, Georgia.
- Scheibling, R. E., Hennigar, A. W., Balch, T., 1999. Destructive grazing, epi-
458 phytism, and disease: the dynamics of sea urchin - kelp interactions in Nova
Scotia. Can. J. Fish. Aquat. Sci./J. can. sci. halieut. aquat. 56, 2300–2314.
- 460 Stoner, A. W., 1989. Winter mass migration of juvenile queen conch *Strombus*
gigas and their influence on the benthic environment. Mar. Ecol. Prog. Ser.
462 56, 99–104.
- Stoner, A. W., Lally, J., 1994. High-density aggregation in queen conch *Strom-*
464 *bus gigas*: formation, patterns, and ecological significance. Mar. Ecol. Prog.
Ser. 106, 73–84.
- 466 Turchin, P., 1998. Quantitative analysis of movement. Sinauer, Sunderland.
- Vadas, R. L., Elner, R. W., Garwood, P. E., Babb, I. G., 1986. Experimen-
468 tal evaluation of aggregation behavior in the sea urchin *Strongylocentrotus*
droebachiensis. Mar. Biol. 90, 433–448.
- 470 Wright, J. T., Dworjanyn, S. A., Rogers, C. N., Steinberg, P. D., Williamson,
J. E., Poore, A. G. B., 2005. Density-dependent sea urchin grazing : differ-
472 ential removal of species, changes in community composition and alternative
community states. Mar. Ecol. 198, 143–156.